



HAL
open science

Sol/gel transition of thermoresponsive Hyaluronan: From liquids to elastic and sticky materials

L. Barbier, M. Protat, P. Pipart, A. Marcellan, Y. Tran, D. Hourdet

► **To cite this version:**

L. Barbier, M. Protat, P. Pipart, A. Marcellan, Y. Tran, et al.. Sol/gel transition of thermoresponsive Hyaluronan: From liquids to elastic and sticky materials. *Carbohydrate Polymers*, 2023, 310, pp.120715. 10.1016/j.carbpol.2023.120715 . hal-04216298

HAL Id: hal-04216298

<https://hal.science/hal-04216298>

Submitted on 25 Sep 2023

HAL is a multi-disciplinary open access archive for the deposit and dissemination of scientific research documents, whether they are published or not. The documents may come from teaching and research institutions in France or abroad, or from public or private research centers.

L'archive ouverte pluridisciplinaire **HAL**, est destinée au dépôt et à la diffusion de documents scientifiques de niveau recherche, publiés ou non, émanant des établissements d'enseignement et de recherche français ou étrangers, des laboratoires publics ou privés.

Sol/gel transition of thermoresponsive Hyaluronan: from liquids to elastic and sticky materials

L. Barbier, M. Protat, P. Pipart, A. Marcellan, Y. Tran, D. Hourdet

Soft Matter Sciences and Engineering, ESPCI Paris, PSL University,
Sorbonne University, CNRS, F-75005 Paris, France

Email addresses: lucile.barbier@espci.fr, mprotat@hotmail.com, perrine.pipart@espci.fr,
alba.marcellan@espci.fr, yvette.tran@espci.fr, dominique.hourdet@espci.fr

Abstract

Thermoassociating copolymers were prepared by grafting temperature responsive poly(*N*-isopropylacrylamide-*stat-N-tert*-butylacrylamide) telomers onto hyaluronan. By varying the composition of LCST side chains, from 50 to 100 wt% of NIPAM units, it is shown that the sol/gel transition of entangled solutions can be accurately controlled in the range of 10 to 35 °C with an abrupt transition and reversible properties. Complementary experiments, performed by DSC and NMR, demonstrate the close relationship between thermoassociation of LCST grafts, forming microdomains of low mobility, and macroscopic properties. Moreover, by performing tack experiments during heating we demonstrate that hyaluronan formulations abruptly switch from a weak adhesive viscous behavior to an elastic adhesive profile in the gel regime. As LCST side-chains form concentrated micro-domains of low mobility, physical gels can resist to dissociation above their sol/gel transition for relatively long periods when immersed in excess physiological medium. The thermoassociative behavior of these copolymers, whose properties can be finely tuned in order to form sticky gels at body temperature, clearly demonstrates their potential in biomedical applications such as injectable gels for drug delivery or tissue engineering.

Keywords: Hyaluronan, hydrogel, tissue engineering, thermo-responsive polymers, gelation.

1. Introduction

Thermo-responsive polymers have attracted considerable attention during the last 30 years as they can be easily used to design smart macromolecular architectures able to reversibly self-assemble in aqueous media. In this context, and depending on the application, the transition temperature (T_{as}) and the extent of the phase separation (from micro to macro) are two relevant parameters that are directly related to the macromolecular design.

Concerning the association temperature, the adequate responsive trigger can be easily selected from the wide list of polymers having a Lower Critical Solution Temperature (LCST) in water like N-substituted poly(acrylamide)s, poly(N-vinyl amide)s, poly(oxazoline)s, poly(ether)s, or poly(oligo(ethylene glycol)methacrylate) (POEGMA)(Aseyev, Tenhu, & Winnik, 2011). This non exhaustive selection is clearly limitless if we consider the possibility to tune the “LCST” of a macromolecular chain by introducing more hydrophilic or hydrophobic comonomers(Durand & Hourdet, 2000; Liu & Zhu, 1999). Once chosen the LCST trigger, the self-assembling remains the central feature as it tightly correlates the macromolecular architecture to the macroscopic properties.

During the 80's, there were a lot of theoretical and experimental works on LCST hydrogels and particularly on poly(*N*-isopropylacrylamide) [PNIPAM], concerning the swelling/collapse behavior induced by temperature or other external parameters like salt, pH, added surfactant or co-solvent(Irie, 1993; Kokufuta, Zhang, Tanaka, & Mamada, 1993; Shibayama, Ikkai, Inamoto, Nomura, & Han, 1996; Suzuki, 1993; Zhang, Tanaka, & Shibayama, 1992). In this case, similar to the coil/globule transition of a single macromolecule, researchers at that time were mainly interested in the volume transition of polymeric materials and to a lesser extent in the mechanical transition induced in isochoric conditions(Shibayama, Morimoto, & Nomura, 1994). With respect to solutions, it is often necessary to maintain the integrity of the formulation and to avoid a macroscopic phase separation at high temperature. For that purpose, the responsive polymer has to be introduced sequentially within the water-soluble structure in order to stabilize the phase separation at a microscopic level. This concept of thermo-associating or thermo-thickening

copolymers, initially developed with cellulosic derivatives(Desbrieres, Hirrien, & Ross-Murphy, 2000; Heymann, 1935; Suto, Nishibori, Kudo, & Karasawa, 1989), have been expanded since with synthetic block copolymers of poly(ethylene oxide) [PEO] and poly(propylene oxide) [PPO](Brown, Schillen, & Hvidt, 1992; Mortensen, Brown, & Jorgensen, 1994) (plurionics) and then explicitly rationalized with graft copolymers tailored with LCST side-chains(Bromberg, 1998; Hourdet, Durand, & Herve, 1999; Hourdet et al., 1998; Hourdet, Lalloret, & Audebert, 1994). When responsive sequences and water-soluble counterparts are well-balanced within the macromolecular architecture, a physical network can be formed and remain stable without syneresis, even at high temperature, provided that the concentration is high enough to allow percolation through the whole volume of the solution. These responsive copolymers are of great interest as they provide technological responses for complex fluids which require improved rheological properties above a given temperature. This situation typically concerns a wide range of industrial formulations like suspensions, coatings(Yeung, Liu, Langlois, Charmot, & Corpart, 2001), cosmetics(L'Alloret, 2006), drilling fluids(Maroy, Hourdet, L'Alloret, & Audebert, 1998) but also biomedical applications(Bellotti, Schilling, Little, & Decuzzi, 2021; Thambi, Phan, & Lee, 2016).

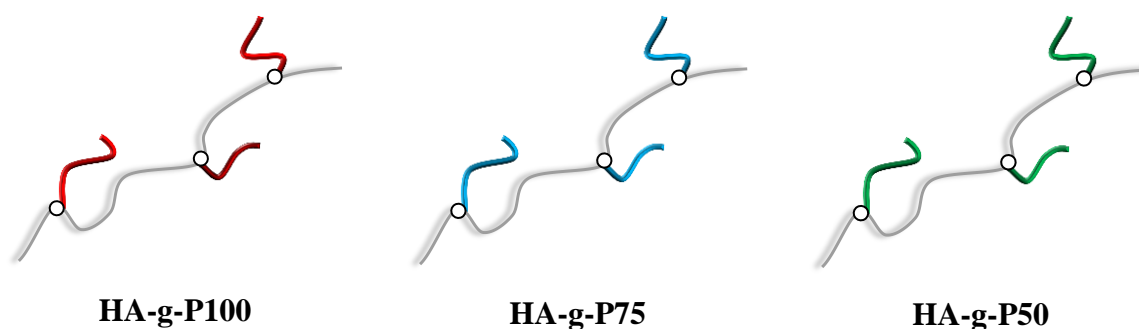
In this field, the concept of injectable hydrogels, that are liquid solutions able to form gel at body temperature, is a crucial issue for specific applications. For instance, the possibility to easily inject active molecules initially embedded into liquid formulations able to form gels spontaneously in contact with physiological surfaces, like buccal(Zeng et al., 2017), ocular(Destruel, Zeng, Maury, Mignet, & Boudy, 2017), vaginal(Bouttier et al., 2020), rectal(Koffi, Agnely, Ponchel, & Grossiord, 2006), nasal(Cao, Yan, Hu, & Zhou, 2015) or gastrointestinal mucosa(Miura et al., 2021), or to protect these surfaces, is clearly a hot topic in drug delivery. In this framework, plurionics, also known as poloxamers, which are FDA approved polymers able to transit from sol to gel in the vicinity of body temperature, are often used as injectable hydrogels Nevertheless they are usually formulated with other polymer, generally polysaccharides, as plurionics exhibit weak mucoadhesive properties(Koffi et al., 2006; Smart, 2005).

In tissue regeneration, the possibility to inject liquid formulations containing cells or drugs that will switch to gel in physiological conditions without any chemical reaction is clearly a challenging topic. In this context, responsive hydrogels also need to mimic the chemical and physical environments of the extracellular matrix (ECM) and natural polymers like proteins (collagen, gelatin, fibrin) or polysaccharides (carboxymethylcellulose, chitosan, alginate and hyaluronan) are very good candidates for these applications(Boateng, Matthews, Stevens, & Eccleston, 2008; Malafaya, Silva, & Reis, 2007).

In this context, the use of PNIPAM derivatives as LCST triggers, is very common and versatile as the incorporation of more hydrophobic monomer, such as NtBAM(Iatridi, Saravanou, & Tsitsilianis, 2019; Muramatsu, Saito, Wada, Hirai, & Miyawaki, 2012; Safakas, Saravanou, Iatridi, & Tsitsilianis, 2021), or more hydrophilic one such as acrylamide(Durand & Hourdet, 2000), allows fine control of the association temperature below or above 32 °C, respectively. Among previous biopolymers, hyaluronic acid (HA), that is one of the main component of ECM in connective, epithelial and neural tissues, clearly appears as a standard and various covalent structures coupling HA to LCST polymers have been developed during the last decade. Different chemistries have been used for this purpose, generally involving covalent coupling between HA and end-functionalized LCST chains(D'Este, Alini, & Eglin, 2012; Ekerdt et al., 2018; Ha et al., 2006; Mortisen, Peroglio, Alini, & Eglin, 2010; Muramatsu et al., 2012), or graft polymerization on modified HA(Ohya, Nakayama, & Matsuda, 2001; Pitarresi, Fiorica, Licciardi, Palumbo, & Giammona, 2013), and various architectures based on HA grafted with PNIPAM, PEGMA(Pitarresi et al., 2013), poloxamers(Ramya, Kodavaty, Dorishetty, Setti, & Deshpande, 2019) or statistic copolymers of ethylene oxide and propylene oxide(D'Este et al., 2012) have been designed with a wide panel of thermo-thickening properties and applications like differentiation of human mesenchymal stem cells, cartilage regeneration(Muramatsu et al., 2012) (repair) or cell-based therapy in disc repair(D'Este et al., 2016; M. Peroglio, Eglin, Benneker, Alini, & Grad, 2013; Marianna Peroglio et al., 2012; Rosenzweig et al., 2018).

Depending on the application, a wide range of specifications are required such as 1) low viscosity below body temperature to inject the formulation, 2) sol/gel transition just below body temperature with thermodynamic and kinetic control of the phase transition, 3) specific gel properties including elastic modulus, deformability, adhesiveness, swelling and stability in physiological environment and 4) biocompatibility and biodegradability.

In this context, our main motivation was to develop a comprehensive study of injectable hydrogels based on hyaluronan grafted with different LCST side-chains in order to investigate their impact on the association behavior and the gel properties. To this end, we designed 3 graft copolymers of similar topology (see **Scheme 1**) starting from a long Hyaluronan backbone and shorter side chains (about one tenth of the Hyaluronan molar mass).



Scheme 1. Schematic representation of graft copolymers designed from the same Hyaluronan backbone (**HA**) and different LCST side-chains (**P_x**) of similar molar masses. The side-chains, **P_x**, were prepared by copolymerization between *N*-isopropylacrylamide (NIPAM) and *N*-*tert*-butylacrylamide (NtBAM), with **x** corresponding to the weight fraction of NIPAM.

By synthesizing these copolymers with equivalent mass fractions of backbone and side chains, this design makes it possible to obtain graft copolymers with a sufficient number of responsive grafts capable of developing efficient associative properties. For that purpose, we prepare a series of LCST copolymers by copolymerization of NIPAM with *N*-*tert*-butylacrylamide (NtBAM) in order to tune the transition temperature below body temperature, typically between 10 and 30 °C. After grafting the LCST polymer onto the hyaluronan backbone, we will investigate the effect of grafting on the transition temperature (T_{as}) and the influence of polymer concentration on the sol/gel transition with respect to the regime of concentration. The viscoelastic behavior will be discussed in relation to current theories on associating polymers. Gel properties will be explored

further, either beyond the linear regime by probing the adhesive behavior in the course of the transition, but also in long term experiments to investigate their swelling properties as well as their stability under physiological conditions.

2. Experimental section

2.1. Reagents and solvents

N-isopropylacrylamide (NIPAM, Aldrich), *N*-*tert*-butylacrylamide (NtBAM, Aldrich), cysteamine hydrochloride (AET, Sigma), potassium peroxydisulfate (KPS, Acros), 1-[3-dimethylaminopropyl]-3-ethylcarbodiimide hydrochloride (EDC, 98%, Acros), *N*-hydroxysuccinimide (NHS, 98%, Aldrich) were used as received without further purification. Water was purified with a Millipore system combining inverse osmosis membrane (Milli RO) and ion exchange resins (Milli Q).

2.2. Polymer precursors

2.2.1. Hyaluronan backbone.

A Hyaluronan sample (**HA**) was purchased from Soliance (France). The number average molar mass, characterized by Size Exclusion Chromatography, was $M_n = 200$ kg/mol with a dispersity of molar masses $\mathcal{D} \cong 2$.

2.2.2. Amino-terminated P(NIPAM-*stat*-NTBAM)

The synthesis of functional chains was carried out by telomerization, which allows controlling the polymer end-group as well as its molar mass. The same protocol detailed in reference (Durand & Hourdet, 1999) was applied for the three copolymers taking care that the reaction takes place below or around 5 °C under nitrogen atmosphere. As NtBAM is less soluble in water than NIPAM, its copolymerization was carried out in more dilute conditions (see **Table 1**). The synthesis of cotelomers can be summarized as follows in the case of PNIPAM: in a three necked flask, 15.3 g of NIPAM (135 mmol) was dissolved in 135 mL of water and the solution was deoxygenated for 1 h with nitrogen bubbling in an iced bath. Redox initiators, KPS (0.37 g; 1.35

mmol) and AET, HCl (0.31 g; 2.7 mmol), were separately dissolved in 10 mL and 5 mL of water, respectively, before addition to the monomer solution. The reaction was allowed to proceed at low temperature, below 5 °C in order to avoid phase separation of the copolymer. After 4 hours, an appropriate amount of sodium hydroxide was added to neutralize ammonium end-groups and the polymer was recovered by dialysis against pure water and freeze-dried. Three PNIPAM copolymers were prepared in these conditions, with an initial weight feed of NIPAM (x) of 100, 75 and 50 wt% (see **Table 1**). The copolymers will be named Px, with x the weight percentage of NIPAM in the copolymer. The synthesis yield after dialysis was between 65-85 wt% for all the reactions. Composition and molar mass of the copolymers were obtained by titration, ¹H NMR and SEC.

| Table 1. Synthesis of amino-terminated P(NIPAM-co-NtBAM) | | | | | |
|---|------------------------------|--------------|--|------------------------|------------------------|
| Telomers | ^a [NIPAM]/[NtBAM] | | ^b [M] ₀ =[Monomer] | [AET]/[M] ₀ | [KPS]/[M] ₀ |
| | Molar ratio | Weight ratio | mol.L ⁻¹ | Molar ratio | Molar ratio |
| P100 | 100/0 | 100/0 | 0.90 | 0.02 | 0.01 |
| P75 | 77/23 | 75/25 | 0.26 | 0.02 | 0.01 |
| P50 | 53/47 | 50/50 | 0.13 | 0.02 | 0.01 |

^a[NIPAM]/[NtBAM] is the monomer feed ratio and ^b[M]₀ is the total monomer concentration.

2.3. Grafting reaction

The coupling reaction between carboxyl groups of HA and terminal amine of PNIPAM derivatives was carried out in cold water using EDC/NHS as coupling reagents, following the procedure already reported for other synthetic and natural polymers (Durand & Hourdet, 1999; Guo, Goncalves, Ducouret, & Hourdet, 2018; Karakasyan, Lack, Brunel, Maingault, & Hourdet, 2008). A schematic representation of the reaction process is given in **Scheme S1** in supporting information. The same procedure has been followed for all the copolymers except the concentration of polymers which has been slightly reduced for the grafting of P50 and P75 in order to avoid interchain coupling initially observed during the grafting of P100 (see **Table 2**). A typical reaction can be summarized as follows for the grafting of PNIPAM onto HA. In a reaction vessel equipped with a magnetic stirrer, 6 g of HA was initially dissolved under stirring in 200 mL of water for at least 24 hours at room temperature. 6 g of PNIPAM was separately dissolved

in 100 mL of cold water in order to get a homogeneous solution and the pH was adjusted around 5-6 with hydrogen chloride (1 mol/L). After cooling the HA solution in an iced bath at $T = 2-3$ °C, the solution of PNIPAM was slowly added and the pH was controlled again and adjusted to pH 5 to 6, if necessary, while adjusting the total amount of water to 350 mL before reaction. After one hour of mixing under stirring below 10 °C, a series of 5 daily feeds of NHS/EDC, initially dissolved separately in 5 mL of water, were added into the reaction vessel and the reaction was let to proceed for at least 24 hours after the last feed. In these conditions, the total molar ratio $EDC/COOH \geq 1$ with a fixed molar ratio $EDC/NHS = 1.6$. The polymer solution was then purified by dialysis initially against sodium chloride 0.1 mol/L, to remove the large excess of positively charged EDC, and then against pure water before freeze drying. The total feed conditions and the yield of the synthesis are given in **Table 2**.

| Table 2. Synthesis of thermo-responsive Hyaluronan : HA-g-Px. | | | | | | | |
|--|--------|-----|--------|---------|---------|-----------|------------------------|
| Copolymer | Grafts | (g) | HA (g) | EDC (g) | NHS (g) | Water (g) | Yield (%) [*] |
| HA-g-P100 | P100 | 6 | 6 | 3.5 | 1.3 | 400 | 54 |
| HA-g-P75 | P75 | 1 | 1 | 1.3 | 0.5 | 175 | 80 |
| HA-g-P50 | P50 | 1.5 | 1.5 | 1.3 | 0.5 | 150 | 83 |

^{*}After dialysis

2.4. ¹H NMR

Hyaluronan precursors and their derivatives were characterized by ¹H NMR in D₂O (~2 wt%) with a Bruker Avance 400 MHz spectrometer, while LCST copolymers were studied in CDCl₃ (see **Figure S1** in supporting information). For advanced analyses of the temperature-responsive self-assembling behavior of HA-g-PNIPAM₅₀, NMR experiments were performed on a Bruker Avance III HD spectrometer operating at 700 MHz for ¹H, using a standard 5 mm broadband smart probe. Temperature control was achieved by a Bruker BCU II unit and a build in temperature control unit. The following experimental conditions were employed for the variable temperature experiments: 32 transients, 45° flip angle, 2.5 sec acquisition time, 2 sec relaxation delay. The sample was allowed to equilibrate for about 10 minutes at each temperature. The ¹H chemical shifts were referred to residual HOD peak at each temperature [30].

2.5. Size Exclusion Chromatography (SEC)

Hyaluronan precursor (HA) and homoPNIPAM (P100) have been characterized by SEC using a Waters system equipped with three Shodex OH-pak columns equilibrated at $T = 20^{\circ}\text{C}$ in aqueous solution (NaNO_3 0.5 mol/L). A triple detection “viscometry/light scattering/refractometry” allows an absolute characterization of the molar masses after an initial calibration of the columns with PEO standards. The two other PNIPAM copolymers (P50 and P75) were characterized similarly by SEC in THF.

2.6. Preparation of copolymer solutions

All studies were performed in the semi-dilute regime, either in pure water or in physiological conditions using phosphate buffer saline (PBS) solutions. For each solution, copolymer and solvent were weighted, mixed and let to dissolve under magnetic stirring in a cold bath until homogenous solutions were obtained. Then, samples were stored between 1 to 5 days in the fridge prior to analysis. Polymer concentrations are given in weight percentage (wt%).

2.7. Linear rheology

Viscoelastic properties of graft copolymers in aqueous solutions were studied in the semi-dilute regime using a stress-controlled rheometer (Haake RS600) equipped with a cone/plate sanded geometry (diameter 35 mm, angle 2° , truncature 103 μm). Experiments were performed in the linear viscoelastic regime which was determined for each sample after various stress sweep and frequency sweep experiments performed at different temperatures: 10, 37 and 60 $^{\circ}\text{C}$ (see **Figure S2**). A particular care was taken to avoid drying of the sample by using a homemade cover which prevents from water evaporation during experiment. Temperature scanning experiments were performed at constant frequency (1 Hz) and shear stress (2 Pa) by applying consecutive heating and cooling scans at $2^{\circ}\text{C}\cdot\text{min}^{-1}$ with a high power Peltier system that provided fast and accurate adjustment of the temperature. In these conditions, storage (G') and loss (G'') moduli (see **Figure**

S3) as well as complex viscosity (η^*) were recorded between 2-10 and 50-60°C according to the sample. Reproducibility was verified for each experiment.

2.8. Probe Tack Test.

Probe tack experiments were adapted from the original work of Vahdati et al. (Vahdati, Ducouret, Creton, & Hourdet, 2020a) using a DHR-3 rheometer (TA Instruments). Using stainless steel surface as simple model, tack tests were performed between a top flat sand-blasted probe ($a_0 = 4\pi r_0^2$ with $r_0 = 10$ mm), attached to the axial load cell of the rheometer, and a bottom sand-blasted plate mounted on the Peltier temperature control system. Initially set at low temperature, a precise volume of liquid polymer solution has been carefully deposited with a micropipette on the bottom plate and the probe was then brought into intimate contact by squeezing the solution to the initial thickness ($h_0 = 400$ μm). The layer was then heated rapidly to the target temperature, followed by a 10 min standing time to make sure that temperature is homogeneous across the sample. The axial force (F) required to detach the probe at a constant debonding rate ($v = 100$ $\mu\text{m}\cdot\text{s}^{-1}$) was recorded as a function of time (t) or displacement (h). Finally, nominal stress ($\sigma = F/a_0$) was plotted versus nominal strain ($\varepsilon = (h - h_0)/h_0$) and work of adhesion (W_{adh}) was calculated from the product of the initial thickness and the area under nominal stress-strain curves up to failure: $W_{adh} = h_0 \times \int_0^{\varepsilon_{\max}} \sigma(\varepsilon) d\varepsilon$. All the probe tack tests were performed at least twice.

2.9. Swelling experiments

In order to get information about the stability of physical gels in aqueous environments, swelling experiments were carried out with HA-g-P100 and HA-g-P50 in the gel state. After thermal equilibration during 15 minutes at $T = 37$ °C for HA-g-P50 (or 50 °C for HA-g-P100) in a plastic syringe, a piece of cylindrical gel was weighted ($m_0 = m_{p,0}/w_p$), with $m_{p,0}$ the initial mass of polymer in the piece of gel and w_p the initial weight fraction of polymer, before being immersed in a large excess of water or PBS solution also at 37 °C (or 50 °C). The sample was then weighted

as a function of time (m_t) and then finally dried in order to estimate the fraction of extractable:

$$w_{ext} = (m_{p,0} - m_{p,t}) / m_{p,0}, \text{ with } m_{p,t} \text{ the mass of polymer in the dried sample.}$$

2.10. Differential Scanning Calorimetry

The phase transition of PNIPAM copolymers in aqueous solution was investigated by Differential Scanning Calorimetry using a DSC Q200 from TA instrument. Polymer solutions (about 80 mg), equilibrated with a reference filled with the same quantity of solvent, were submitted to temperature cycles between -5°C and 60°C . Heating and cooling rates were fixed at $2^{\circ}\text{C}\cdot\text{min}^{-1}$ similarly as the rates used in rheology experiments.

2.11. Injectability

For proof of concept, injectability tests were performed by injecting HA-g-P100 and HA-g-P50 solutions, initially stored below their gelation temperature, into a PBS solution thermostated either below or above the gel point. In order to visually follow the evolution of the solution injected into the PBS bath, Rhodamine B was initially mixed with the polymer solution ($C = 0.01$ wt%). In the case of HA-g-P100 the injection force as a function of flow rate was also determined using a specific setup mounted on an Instron machine (see supporting information).

3. Results and Discussion

3.1. Synthesis and characterization of LCST precursors

As shown in **Table 3**, the three syntheses performed with various compositions of NIPAM/NtBAM, keeping constant telogen (and persulfate)/monomer ratios, give rise to copolymer chains with similar number average molar masses ($M_n = 15\text{-}20$ kg/mol) and moderate dispersity ($\mathcal{D} = 1.2\text{-}1.6$). Moreover, final compositions of the copolymer are almost identical to those of the initial feed ratio as it could be expected since the monomer reactivity ratios are rather close and copolymerization is almost quantitative. This was studied in more detail by Gibbons et

al.(Gibbons, Carroll, Aldabbagh, & Yamada, 2006) who demonstrate that the NIPAM-NtBAM copolymer composition remained similar to the feed ratios regardless of polymerization processes (conventional or controlled) and experimental conditions such as solvent, temperature or conversion. Thermal properties of copolymers have been studied by DSC as the phase separation process of all these LCST copolymers displays a clear endotherm during the heating process corresponding to the reorganization of interactions between monomer units and water molecules. Here, analyses were performed in PBS solution which does not really impact the association temperature as the salting out remains weak in these conditions. As reported in **Figure 1** with P100 solution, the beginning of the phase transition is clearly observed around 33.4 °C with a maximum of the endotherm located at $T_{\max,heat} = 36.8$ °C.

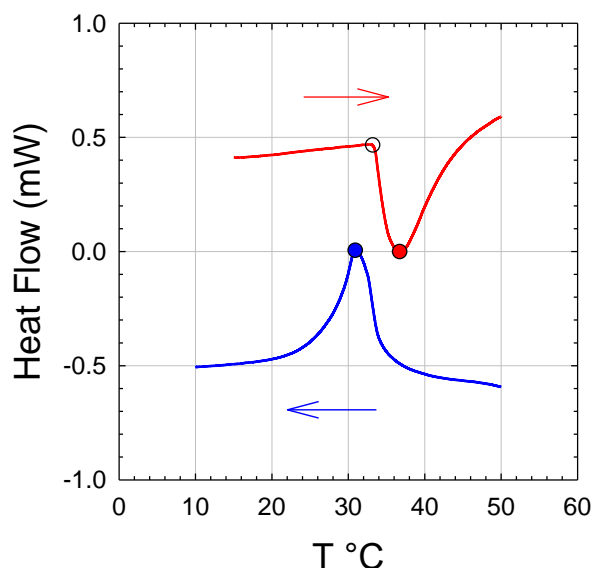


Figure 1

Thermograms of a P100 solution prepared in PBS ($C = 2$ wt%).

T_{on} (○) and $T_{\max/heat}$ (●) denote, respectively, the onset temperature and the temperature at the maximum of the endotherm during heating. $T_{\max/cool}$ (●) denotes the maximum of the exotherm during cooling.

Heating and cooling rates = 2 °C.min⁻¹

By cooling, the remixing of the two phases starts below 38 °C with a maximum of the exotherm located at 31.0 °C. This hysteresis mainly originates from kinetic effect at this rate of cooling, here 2 °C/min, as the PNIPAM chains phase separate into highly concentrated domains of low mobility due to the proximity of their glass transition. This hysteresis can be reduced, even eliminated, when applying much slower sweeping rate, typically below 1 °C/min. The comparison between the 3 LCST Px polymers in **Figure 2** highlights the impact of the hydrophobic modification of the copolymer with a decrease of the transition temperature $T_{\max,heat}$

(see also **Table 4**) with the increasing fraction of hydrophobic NtBAM. At the same time, the hysteresis that can be estimated by the difference between the maxima observed during heating and cooling steps increases from around 6 °C, 10 °C and above for $x = 100, 75$ and 50 . These characteristic temperatures are in perfect agreement with those reported by Hoffman et al. (Hoffman et al., 2000) who have explored NIPAM-NtBAM copolymers over a much broader range of composition going from 100-0 to 30-70 (in mol%). Upon heating, the end of the transition, which can be appreciated from the endotherm, is around 50 °C for P100 but the transition is already achieved at 40 and 30 °C for P75 and P50, respectively.

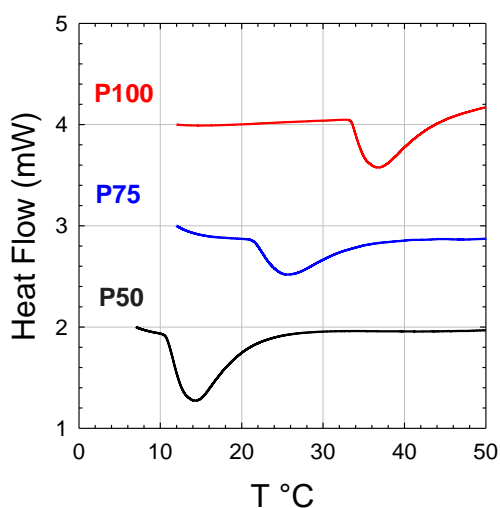


Figure 2

Endotherms of LCST polymer solutions prepared in PBS ($C = 2$ wt%). Heating rate = 2 °C.min⁻¹

For these two copolymers, and especially for the last one (P50), this means that it possible to fully achieve the phase separation process in physiological conditions, which is not the case for P100.

| Table 3. Characteristics of LCST precursors | | | | |
|--|----------------------------|------------------|---|-----------------------------------|
| Grafts | M_n (g/mol) ^a | \mathcal{D} | NIPAM/NtBAM Weight Composition ^b | $T_{\max,heat}$ (°C) ^c |
| P100 | 19 500 | 1.2 ^a | 100/0 | 36.8 |
| P75 | 15 500 | 1.6 ^a | 75/25 | 25.6 |
| P50 | 14 800 | 1.6 ^a | 50/50 | 14.3 |

(a) number average molar mass (M_n) and dispersity of molar masses (\mathcal{D}) obtained from SEC; (b) weight composition of NIPAM and NtBAM comonomers in the copolymer calculated from ¹H NMR; (c) temperature at the maximum of the endothermic peak ($T_{\max,heat}$) determined by DSC with LCST precursors in PBS solutions (2 wt%).

3.2. Synthesis and characterization of graft copolymers

For all the coupling reactions, which were carried out in water, the pH is a key parameter for the formation of amide bonds as it results from a compromise between successive reactions which involve: 1) the reaction of EDC/NHS with carboxyl groups to form O-acylisourea, NHS activated ester or anhydride at $\text{pH} = 3.5\text{-}5$ and 2) the amide formation between previous intermediates and non-ionized amines which prevail at higher pH (Nakajima & Ikada, 1995; Staros, Wright, & Swingle, 1986) (see **Scheme 1** in supporting information). Obviously the ionization equilibrium depends on the pK_a of the amine, but generally it comes that $\text{pH}=5$ is a good compromise between the above mentioned requirements. The grafting reaction proceeding in water, we have also to consider the thermodynamic properties of LCST polymeric grafts. As mentioned previously, the solubility of these precursors varies with their composition but they are all soluble in water below $10\text{ }^\circ\text{C}$ and the reactions were consequently performed in an iced bath at $T = 2\text{-}5\text{ }^\circ\text{C}$ in order to work in homogeneous conditions and to promote the random distribution of LCST grafts along the polysaccharide backbone. The characterization of the copolymers by ^1H NMR (see supporting information **Table S1** and **Figure S1**) shows that the coupling reactions are almost quantitative as the composition of the copolymers roughly corresponds to the feed polymer ratio. The lower weight fraction of HA into the copolymer (45 wt%) compared to the feed ratio (50 wt%) is attributed to the higher level of hydration of HA powder (compared to dry Px) which was not taken into account in the initial weighing of compounds. Even if the copolymer solutions (HA-g-Px) becomes opalescent above their transition temperature, highlighting the presence of residual ungrafted LCST side chains, we can reasonably assume that most of the LCST side-chains have been effectively grafted onto the HA backbone. If we consider the initial number average molar mass of the precursors, these grafting ratio correspond to about 12 and 16 LCST grafts per HA backbone for P100 and P50-P75 respectively. As shown in **Table 2**, the yield after purification is around 80 % for most of the coupling reactions except for HA-g-P100 which has been treated in basic conditions ($\text{pH}=13$) at the end of the reaction. Indeed, after several additions of coupling reagent the reaction medium has shown a weak gel-like behavior that was attributed

to either the formation of ester bonds between carboxyl and hydroxyl groups of hyaluronic chains (Neises & Steglich, 1978) or to anhydride bridges between hyaluronan chains (Hermanson, 1996). The formation of such covalent bonds, that we have already observed when adding large amounts of EDC/NHS to alginate solutions for instance, can be readily hydrolyzed in basic medium.

3.3. Thermoresponsive behavior of modified Hyaluronans

3.3.1. DSC and NMR analyses

As shown by DSC in **Figure 3**, the incorporation of P100 side chains onto the hyaluronic backbone does not apparently modify the thermodynamic behavior of the LCST polymer as the phase transition takes place on a similar temperature range whether the PNIPAM chains are grafted or not.

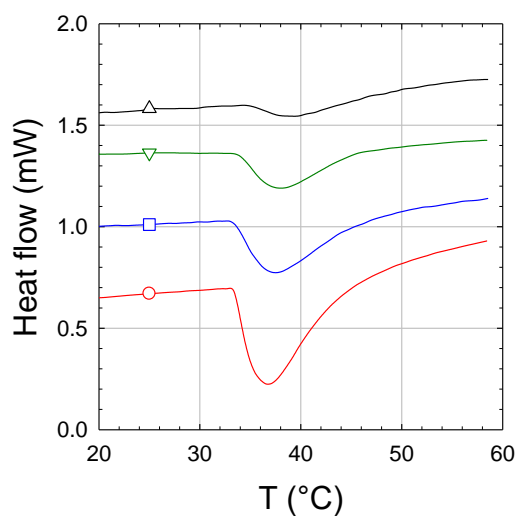


Figure 3

Endotherms of homoPNIPAM (P100) and HA-g-P100 solutions prepared in PBS at different concentrations.
Heating rate = 2 °C.min⁻¹
P100 at 2 wt% (○) and HA-g-P100 at 1.5 wt% (△), 3 wt% (▽) and 5 wt% (□)

While the transition temperatures are similar, the main difference arises from the transition enthalpy, expressed in kJ per mol of NIPAM unit, which is almost two times lower for the graft copolymer compared to the homoPNIPAM precursor (see **Table 4**). This behavior that has been observed with a lot of similar systems (Karakasyan et al., 2008; Vahdati, Ducouret, Creton, & Hourdet, 2020b) can be explained by considering that the transition enthalpy is correlated to the effective balance between disruption (water-amide) and reformation (water-water and amide-

amide) of hydrogen bonds. The lower energy observed for the aggregation of PNIPAM chains covalently bound to the hyaluronic backbone could be related to (1) the energy barrier against the association process due to the steric hindrance imposed by the water-soluble backbone and/or (2) to the formation of smaller and/or less dehydrated PNIPAM aggregates at high temperature. As shown in **Figure S4**, in supplementary information, as well as in **Table 4**, the same conclusions hold for the two other copolymers grafted with P75 and P50.

| Polymer | C wt% | DSC* | | | Rheology* | | | |
|-----------|-------|---------------------|---------------|----------------|---------------|----------------|----------------------------|-----------------------|
| | | ΔH (kJ/mol) | T_{as} (°C) | T_{max} (°C) | T_{as} (°C) | T_{gel} (°C) | $\eta_{6^\circ C}$ (mPa.s) | $G_{50^\circ C}$ (Pa) |
| P100 | 2.0 | 6.5 | 33.4 | 36.8 | | | | |
| HA-g-P100 | 1.5 | 2.5 | 34.9 | 39.6 | 34.1 | 37.1 | 59 | 81 |
| HA-g-P100 | 3.0 | 2.9 | 33.9 | 38.0 | 33.7 | 36.2 | 464 | 346 |
| HA-g-P100 | 5.0 | 3.1 | 33.5 | 37.6 | 32.1 | 35.2 | 3080 | 928 |
| P75 | 2.0 | 5.4 | 21.5 | 25.6 | | | | |
| HA-g-P75 | 1.5 | 3.7 | 22.6 | 26.9 | 18.2 | 24.7 | 210 | 252 |
| HA-g-P75 | 3.0 | 3.8 | 21.7 | 25.8 | 19.1 | 23.1 | 1960 | 951 |
| HA-g-P75 | 5.0 | 4.3 | 21.1 | 25.7 | 18.7 | 19.2 | 12370 | 2382 |
| P50 | 2.0 | 8.8 | 10.7 | 14.3 | | | | |
| HA-g-P50 | 1.5 | 5.1 | 11.6 | 15.4 | 10.7 | 12.7 | 136 | 176 |
| HA-g-P50 | 3.0 | 6.1 | 11.0 | 14.9 | 9.7 | 12.3 | 1110 | 462 |
| HA-g-P50 | 5.0 | 6.0 | 10.0 | 14.0 | 8.7 | 10.3 | 11400 | 2038 |

* All data were determined during the heating step

Complementary experiments were carried out by 1H NMR with the copolymer HA-g-P50 to investigate the aggregation process of LCST side-chains as a function of temperature. From the series of NMR spectra obtained between 4 and 45 °C with a copolymer solution at 1.5 wt% in D₂O (**Figure 4**), we can see that the signals of methyl protons of NIPAM and NtBAM units, observed at about 1.1 and 1.3 ppm respectively, as well as the methanetriyl proton of NIPAM at about 3.9 ppm, show a dramatic decrease above 10 °C. Conversely, the proton signal of the hyaluronan cycle remains almost unaffected by the temperature change as clearly highlighted in **Figure 4b** where the normalized area of protons signals has been plotted as a function of temperature. At 45 °C, the remaining proton signals of LCST side-chains is less than 10% from the value determined at 4 °C, below the transition temperature. This feature, that has been

reported with PNIPAM copolymers (Guo et al., 2015) and gels (Sun et al., 2003), can be assigned to the formation of a solid-like rich-polymer phase with highly reduced mobility. As shown in **Figure 4**, the peaks of hyaluronic backbone are still observable at high temperature although the gel-like behavior of the formulation highly broadens the respective signals. The main conclusion that holds by coupling DSC and NMR data is that at high temperature most of LCST sequences are aggregated into polymer-rich domains of low mobility from the NMR point of view. The low exchange rate of P(NIPAM-co-NtBAM) sequences at high temperature will have a strong impact on the dynamic properties of the copolymer assemblies.

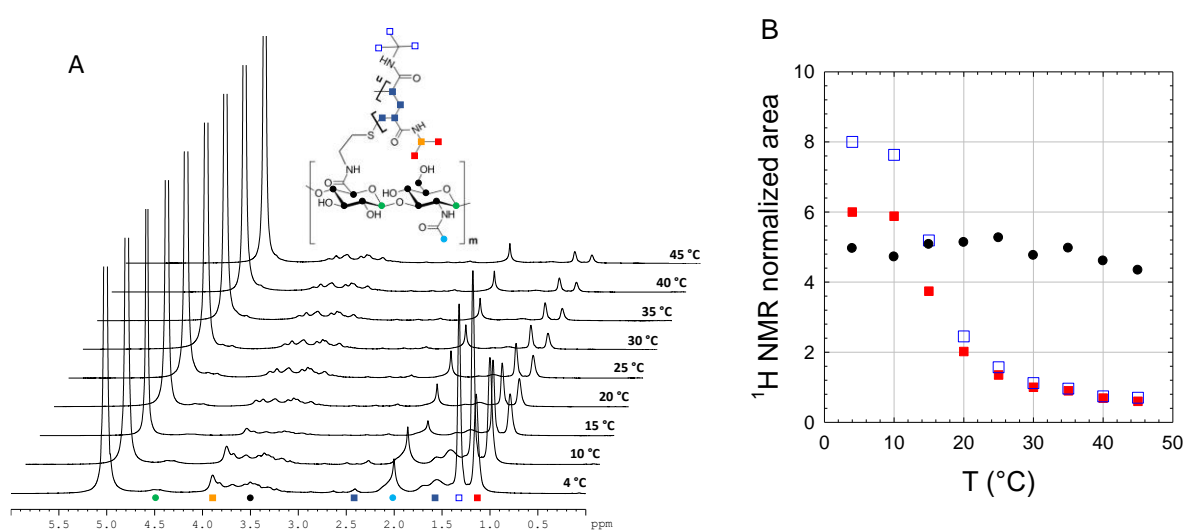


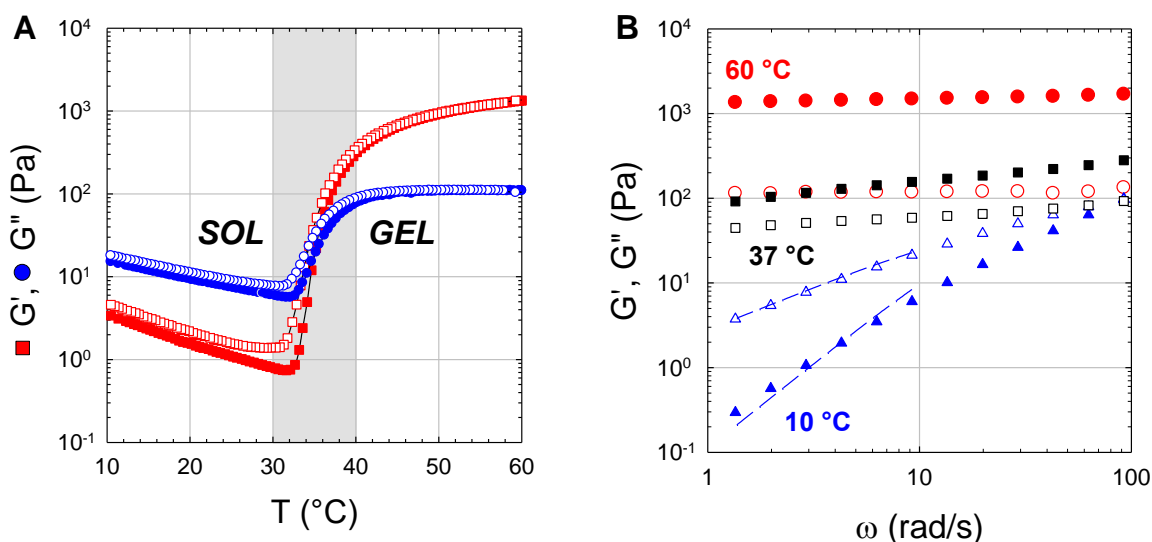
Figure 4. **A)** ¹H NMR spectra of HA-g-P50 solution (1.5 wt%) performed at different temperatures with the main attributions of the peaks. **B)** Temperature dependence of the normalized area corresponding to the methyl protons of NIPAM (■) and NtBAM (□) and to the methanetriyl protons of hyaluronan cycle (● $\delta = 3.0\text{-}4.2$ ppm after subtracting the contribution due to CH protons of NIPAM).

3.3.2. Viscoelastic properties in the linear regime

Strongly coupled to the thermodynamic properties, the viscoelastic behavior of semi-dilute solutions of HA-g-Px nicely mirror the microphase separation giving rise to the formation of physical crosslinks. A representative example is given in **Figure 5** with a 5 wt% HA-g-P100 solution, where variations of dynamic moduli (G' and G'') have been plotted as a function of temperature, for a given frequency (1 Hz), or as a function of the frequency at three different temperatures. After an initial decrease of the viscoelastic properties with increasing temperature, which follows the classical Arrhenius dependence, both G' and G'' sharply increase at about

32°C, highlighting the beginning of the association process which closely corresponds to the transition temperature of PNIPAM side-chains determined by DSC (see **Table 4**). This sol/gel transition, which takes place between 30 and 40°C with the crossover of dynamic moduli, is then followed by a weaker temperature dependence above 40°C, in the gel regime. In **Figure 5B**, the corresponding frequency dependences clearly underline the sol/gel transition starting from a viscous liquid state at low temperature, here 10°C ($G' \sim \omega^2$ and $G'' \sim \omega$), and reaching an elastic gel state at high temperature (60°C) with almost no frequency dependence for both dynamic moduli. In between, like at 37°C, the formulation passes through intermediate states pointing out the existence of a gel point. In our case, the gelation temperature (T_{gel}) is defined by the crossover of dynamic moduli determined at fixed frequency, here $f = 1$ Hz, that is very close in this case to the body temperature (see **Table 4**). This transition is sharp and fully reversible with little hysteresis as already pointed out from the thermodynamic properties of the grafts.

Figure 5. (A) Variation of viscoelastic moduli (G' : ■□ and G'' ●○) of HA-g-P100 in PBS ($C_p = 5$ wt%; $f = 1$ Hz) upon heating (close symbols) and cooling (open symbols), (B) Frequency dependence of the same formulation at 3 different temperatures : 10, 37 and 60°C.



In order to analyse the rheological behavior, viscoelastic data have been replotted by using the complex viscosity (η^*) as a single parameter (see **Figure 6**). Indeed, $\eta^* = \sqrt{(G'/\omega)^2 + (G''/\omega)^2}$ can be identified to the Newtonian viscosity in the sol regime ($\eta^* \cong \eta_0$, for $G'' \gg G'$), while it

scales with the plateau modulus (G_0) in the gel regime for $G' \gg G''$: $\eta^* \cong G_0/\omega$, with $\omega = 6.28$ rad/s in our experimental conditions. As shown in **Figure 6**, the association of PNIPAM side-chains above their transition temperature gives rise to abrupt changes of η^* leading to a large variation of viscosity. As the complex viscosity inversely scales with the frequency in the gel regime, $\eta^* \cong G_0/\omega$, a second y-axis has also been added on the right to highlight the values of the elastic modulus which is constant, at least in the frequency window explored. By comparison with these dynamic experiments carried out at low deformation in the linear regime, the steady state shear viscosity ($\eta_{\dot{\gamma}}$) was analysed in similar condition ($\dot{\gamma} = 6.28 \text{ s}^{-1}$). While the equivalence $\eta_{\dot{\gamma}} = \eta_{\omega}$ is well observed below T_{gel} the steady state shear viscosity starts to diverge in the high temperature range, above 40°C (see SI **Figure S5**). Even if the empirical Cox-Merz rule ($\eta_{\omega}^* = \eta_{\dot{\gamma}}$) has been found to hold for polymer melts, and concentrated or semi-dilute solutions, this relation generally fails with colloidal or gelled systems due to a larger loss of structure at high deformations (Alhadithi et al., 1992). This loss of viscoelastic properties under shear is nevertheless reversible and the gel material demonstrate self-healing properties with time at high temperature or by applying a cooling/heating cycle as shown in **Figure S5**.

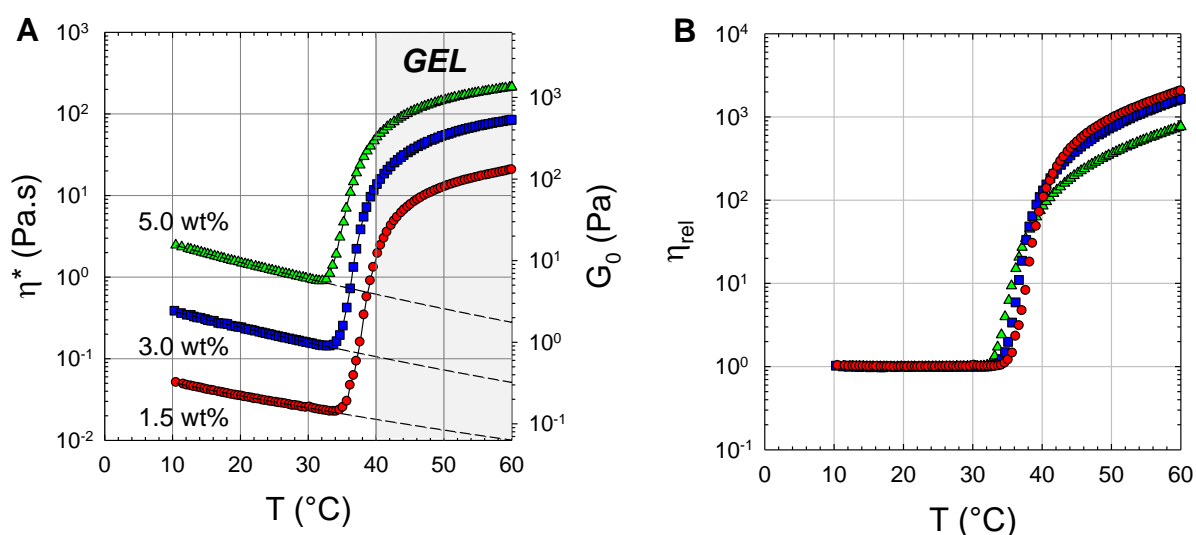


Figure 6. (A) Temperature dependence of complex viscosity (η^*) of HA-g-P100 solutions prepared in PBS at $C = 1.5$ wt% (●); 3 wt% (■) and 5 wt% (▲). The viscoelastic analysis has been performed at fixed frequency ($f = 1$ Hz or $\omega = 6.28$ rad/s). The corresponding scale for the elastic modulus reported on the right axis ($G_0 \cong 6.28 \cdot \eta^*$), is valid only in the gel regime; typically above 40°C for the 3 polymer solutions. The dashed line corresponds to the Arrhenius fit of η^* versus temperature in the sol regime (η_{sol}^*). (B) Temperature dependence of the relative viscosity: ($\eta_{\text{rel}} = \eta^*/\eta_{\text{sol}}^*$).

From a general point of view, the temperature dependence of the complex viscosity can be interestingly normalized by dividing η^* by the Newtonian viscosity (η_{sol}^*) of the unassociated polymer solution: $\eta_{rel}^* = \eta^*/\eta_{sol}^*$. For that purpose, experimental data obtained in the sol regime have been fitted by the Andrade equation: $\eta_{sol}^* = A \cdot \exp(E_a/RT)$ in order to extrapolate the Newtonian viscosity in the whole temperature range: between 10 and 60 °C (see **Figure 6A**). For all hyaluronan solutions investigated in this study, the activation energy for viscous flow calculated in the sol regime was $E_a = 27 \pm 6 \text{ kJ/mol}$; typical of nonassociating polymer solutions in this range of concentrations. As shown in **Figure 6B**, the plot of the relative viscosity clearly emphasizes the association process with the baseline corresponding to the “sol” domain (unassociating polymer chains) and a large increase of the relative viscosity as soon as the association mechanism takes place, leading to the physical gelation of the solution with an amplification factor (η_{rel}) of about 3 decades at 60°C. This normalized curve is systematically used to define the beginning of the association process observed during heating (T_{as}), taking $\eta_{rel} = 1.1$ (10% deviation over more than 1000%) as criterion. While the transition temperature is an intrinsic property of the LCST graft, the thermo-thickening behaviour, i.e. the initial viscosity at low temperature and the elastic modulus above the transition temperature, can be adjusted with the polymer concentration. As shown in **Figure 6**, the variation of complex viscosity upon heating display almost the same signature for the 3 polymer concentrations investigated with very close self-association temperature, in good agreement with DSC data (see **Table 4**), and a shift of the rheological properties towards higher values. Comparatively, the association temperature can be readily controlled through the thermodynamic properties of LCST side-chains. As shown in **Figure 7** and **Table 4** (see also **Figure S3**), the association and gelation temperature can be lowered by 15 or 25°C by using the less hydrophilic grafts, P75 and P50, respectively.

Taking into account the whole set of rheological data, several points are worth discussing. First, the solutions of HA-g-P50 display a large hysteresis in the transition zone between heating and cooling steps. This hysteresis, already pointed out by DSC with the P50 precursor, is related to slow dynamics of these polymers above their transition temperature due to the higher content of

bulky and hydrophobic *t*-butyl groups. Such behavior has already been reported by Tsitsilianis and coworkers (Safakas et al., 2021) in the case of alginates grafted with P(NIPAM-co-NtBAM) side chains of various compositions. The other point is related to the lower viscosity of HA-g-P100 solutions compared to those of other grafted hyaluronan below the transition temperature, like at 6°C for instance as reported in **Table 4**.

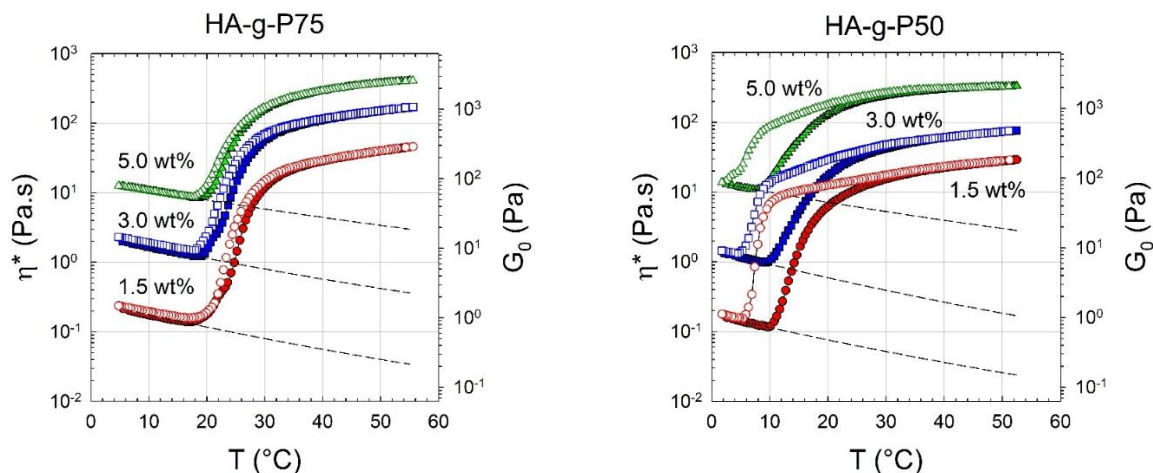


Figure 7. Temperature dependence of the complex viscosity (η^*) of **HA-g-P75** and **HA-g-P50** solutions prepared in PBS at $C = 1.5$ wt% (\bullet \circ); 3 wt% (\blacksquare \square) and 5 wt% (\blacktriangle \triangle). The viscoelastic analysis has been performed at fixed frequency ($f = 1$ Hz or $\omega = 6.28$ rad/s upon heating (close symbols) and cooling (open symbols)). The corresponding scale for the elastic modulus reported on the right axis ($G_0 \cong 6.28 \cdot \eta^*$), is valid only in the gel regime. The dashed line corresponds to the Arrhenius fit of η^* versus temperature in the sol regime (η_{sol}^*).

As mentioned in the synthesis section, some ester crosslinks can be formed during grafting performed in excess of carbodiimide and this has been observed in particular in the case of HA-g-P100 which has been treated with sodium hydroxide ($\text{pH} \cong 13$) to hydrolyze these interchain ester bounds. Although, hyaluronan is quite resistant to hydrolysis we can nevertheless assume that either some additional chain breakage happened during the hydrolysis of HA-g-P100, or conversely that some interchain crosslinks occurred during the grafting process of the two other samples, increasing consequently the average molar mass. If we assume, as we will see below, that all the solutions were studied in the semi-dilute entangled regime, where the viscosity strongly increases theoretically with the molar mass as $\eta \sim M^{3.4}$, the decrease of viscosity between HA-g-P100 and HA-g-P75 or HA-g-P50 corresponds to a decrease of the molar mass ratio by a factor 1.5 or 1.3-1.4, respectively. This statement concerning the entangled regime is clearly

highlighted in **Figure 8** by plotting the Newtonian viscosity determined at 6 °C, in the sol regime, versus the concentration. Indeed, the 3 series of polymer solutions follow a similar scaling relation $\eta \sim C^\alpha$, with $\alpha = 3.5 \pm 0.2$ in rather good agreement with theoretical predictions for semi-dilute entangled neutral polymer solutions in athermal solvent or flexible polyelectrolytes in the high-salt limit ($\eta \sim C^{15/4}$). (Colby, 2010) This is typically the case with HA-g-PX solutions in PBS containing more added salt ions than counterions and similar results ($\eta \sim C^{4.0 \pm 0.2}$) have been reported by Milas et al. (Milas et al., 2001) as well as by Krause et al. (Krause, Bellomo, & Colby, 2001). Moreover, if we consider that the entanglement concentration of polymer solutions (C_e) is typically reached for $\eta \cong 30 \cdot \eta_{solvent}$ (Krause et al., 2001; Milas et al., 2001), which is clearly below all the solutions investigated at $C \geq 1.5$ wt% (see **Table 5**), we can extrapolate this critical concentration at $\eta_{ce} = 0.03$ Pa.s from the plot $\eta = f(C)$ in **Figure 8A**. This gives $C_e = 1.24$, 0.85 and 1.03 wt% for the 3 hyaluronic samples grafted with P100, P75 and P50, respectively. Under the hypothesis of athermal solvent, the concentration dependence of the viscosity can be interestingly reduced either by using the overlap concentration (C^*) or the entanglement concentration (C_e) which are proportional in these conditions (Michael Rubinstein & Colby, 2007). As shown in **Figure 8B**, the plot of the viscosity versus the reduced concentration (C/C_e) gives rise to a single relation in good agreement with the theory.

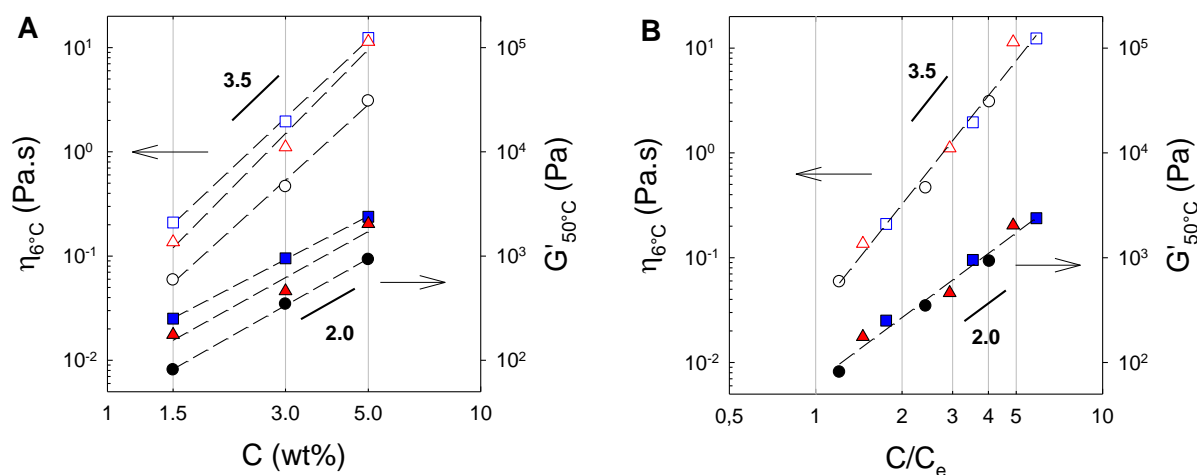


Figure 8 (A) Concentration dependence of Newtonian viscosity ($T = 6$ °C; open symbols) and elastic modulus ($T = 50$ °C; filled symbols) of HA-g-Px solutions in PBS; with $x = 100$ (\circ \bullet), 75 (\square \blacksquare) and 50 (\triangle \blacktriangle). (B) The same data are plotted versus the relative concentration normalized with C_e , the entanglement concentration.

At 50 °C, in the gel regime, the elastic modulus scales as $G \sim C^2$. Such “quadratic” dependence of the modulus with the concentration is relatively common well above the percolation threshold, and it has been widely reported experimentally for many macromolecular physical network and in particular for thermoassociating polymers showing either gelation upon cooling (gelatin, carrageenan, agarose)(A. H. Clark & Farrer, 1995; Allan H. Clark & Ross-Murphy, 1985; Rochas et al., 1989) or upon heating like Bovine Serum Albumine(Allan H. Clark & Ross-Murphy, 1985) and methylcellulose(Arvidson et al., 2013).

In parallel, various theoretical models have been developed to describe the concentration dependence of elastic properties. This is the case for gelation theories based on the pioneering works of Flory(Flory, 1941) and Stockmayer(Stockmayer, 1943), further extended by Hermans(Hermans Jr, 1965) and Clark et al(Allan H. Clark & Ross-Murphy, 1985). Using different assumptions, they show that well above the percolation threshold (C_0), the shear modulus can be described by a scaling relation $G \sim C^\delta$ with $\delta = 2$ in the case of bimolecular interactions or cascade theory taking into account a large number of functional group per chain. A similar quadratic dependence can also be predicted for biphasic copolymer solutions above their transition temperature by analogy with nanocomposites. In this case, the shear modulus of nanocomposites (G_c) can be described by the following expression(Soyarslan, Pradas, & Bargmann, 2019):

$$G_c = G_1 + (G_2 - G_1)\phi_2^2$$

with G_i and ϕ_i , the shear modulus and volume fraction of the soft ($i = 1$) and hard ($i = 2$) phases and $G_c \cong G_2\phi_2^2$ when $G_1 \ll G_2$.

Last but not least, similar scaling relations have been well established for entangled solutions of polymers, associating polymers or loosely crosslinked chemical hydrogels: $G \sim C^\beta$ with $\beta = 9/4$ in athermal solvents(Leibler et al., 1991; Obukhov et al., 1994; Michael Rubinstein & Colby, 2007; M. Rubinstein & Semenov, 2001).

As shown in **Figure 8B**, both the viscosity at low temperature and the elastic modulus at high temperature can be reduced for the 3 grafted hyaluronans by using the entanglement concentration. Although this is not expressly considered in the previous models, the normalization of G' as $G' \sim (C/C_e)^2$, leading to $G' \sim C^2 M^{3/2}$ with $C_e \sim M^{-3/4}$, means that the molecular weight of the polymer chain and its level of entanglement really matter in the final elastic properties of the thermoassociating polymers.

3.3.3. Swelling properties of physical gels

Since the lifetime of the association does not allow to access the dynamics of physical gels their swelling properties were investigated to highlight their long term behavior in the gel state. For that purpose, a 5 wt% solution of HA-g-P50 was initially prepared in PBS at $T = 5^\circ\text{C}$, below the transition temperature. The solution was then introduced into a syringe and heated at 37°C for 15 minutes in an oven. Then, a piece of the cylindrical gel was poured into a closed container filled with a large excess of PBS at 37°C and stored in the oven; the macroscopic gel being regularly weighted with time during 6 days. Gel swelling is calculated as $Q = m_t/m_0$ with m_t the weight of the swollen gel at time t and m_0 the initial weight of polymer in the gel. As shown in **Figure 9**, the physically crosslinked formulation swells moderately in PBS and reach equilibrium after 1 day: from $Q_0 = 20$ to $Q_e = 50$ (or $C_0 = 5 \text{ wt\%}$ to $C_e = 2.0 \text{ wt\%}$).

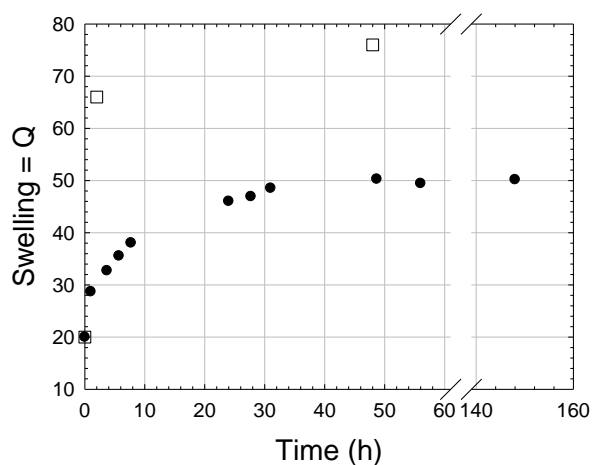


Figure 9

Swelling behavior in the gel state of hyaluronan formulations prepared at 5 wt% in PBS:

- HA-g-P100 ($Q_0 = 20$); $T = 50^\circ\text{C}$
- HA-g-P50 ($Q_0 = 20$); $T = 37^\circ\text{C}$

Throughout the swelling experiment, the swollen network keeps its cylindrical shape and at the end of the study, after drying overnight at 60°C, the polymer loss was shown to be less than 20 wt%. This simple experiment proves that the physical crosslinks formed between LCST side chains are rather strong or more precisely that their dynamics is very slow as most the chains remain connected even after almost 1 week in PBS solution. A similar study was carried out with a 5 wt% HA-g-P100 gel prepared at 50°C in PBS following the same procedure. The results gathered in **Figure 9** clearly highlight a higher level of swelling for HA-g-P100 compared to the previous sample that can be ascribed to a lower level of physical crosslinks: $G'_{50^{\circ}C} = 930 Pa$ for HA-g-P100 against $G'_{37^{\circ}C} = 1760 Pa$ for HA-g-P50 at the same initial concentration of 5 wt% ($Q_0 = 20$). Moreover, if the level of extractible is around 10 wt% after 2 hours, it reaches 35 wt% after 2 days. Even if the results of this swelling study remains qualitative, they clearly underline the very low dynamics of the physical associations which make these gels strong, robust and stable. The lifetime of the whole network in wet environments unquestionably depends on external parameters such as temperature, ionic strength and pH. However other parameters, like the level of entanglements which impact the connectivity, also play a role in the swelling and disruption of the hydrogel.

3.3.4. Adhesive properties of thermoresponsive Hyaluronan.

Adhesive properties of hyaluronan formulations were studied as a function of temperature using a DHR-3 rheometer. In the tack configuration, the liquid sample, in the sol state, was initially confined ($h_0 = 400 \mu m$) between two flat sand-blasted plates; the probe one at the top ($a_0 = 4\pi r_0^2$ with $r_0 = 10 mm$), and the bottom one being mounted on a Peltier temperature control system. The formulation was then equilibrated at a given temperature for 10 minutes before starting the experiment performed at a constant debonding rate $v = 100 \mu m.s^{-1}$, corresponding to $\dot{\lambda} = 0.25 s^{-1}$ in our conditions. As shown in **Figure 10** for the formulation of HA-g-P100 at 5 wt% in PBS, the stress-strain profiles are strongly modified upon heating starting from a viscous

response at low temperature up to a viscoelastic one above the transition. Theoretical fits have been added in supporting information (**Figure S6**) in order to model the theoretical capillary (σ_{cap}), viscous (σ_{η}) and elastic (σ_{G}) contributions given by the following relations(Shull, Creton, Shull, & Creton, 2004):

$$\sigma_{\text{cap}} = \frac{2\gamma}{h_0(\epsilon+1)} \quad [1] \quad \sigma_{\eta} = \frac{3\eta\dot{\lambda}}{(\epsilon+1)^2} \left(1 + \frac{1}{2} \frac{(a_0/h_0)^2}{(\epsilon+1)^3}\right) \quad [2] \quad \sigma_{\text{G}} = 3G\epsilon \left(1 + \frac{1}{2} (a_0/h_0)^2\right) \quad [3]$$

where γ is the surface energy of water ($\gamma = 72$ mN/m in the range $T = 30\text{-}40$ °C) and ϵ is the nominal strain equal to $(h-h_0)/h_0$.

For that purpose, we have used the complex viscosity at low temperature and the elastic modulus at high temperature. At low temperature, below and within the transition zone ($T = 32$ and 37°C), the σ - ϵ curves correspond mostly to a viscous liquid behavior with an initial maximum stress at $\epsilon = 0$ dominated by capillary forces at 32°C ($\sigma_{\text{max}} = 2\gamma/h_0 \cong 350$ Pa) and viscosity at 37°C ($\sigma_{\text{max}} \cong (3/2)\eta\dot{\lambda}(a_0/h_0)^2 \cong 235\eta \cong 680$ Pa). Then the stress decays rapidly versus deformation with forces below the experimental resolution making difficult to accurately define the strain at break and to calculate the work of adhesion. Well above the transition threshold, for $T = 42^\circ\text{C}$ and 46°C , the formulation becomes predominantly elastic and the initial part of the stress-strain curve can be fitted reasonably well with equation [3] which highlights the effect of the confinement over mechanical properties. Then the curve reaches a maximum stress which coincides with the occurrence of fingering instabilities in the periphery of the hydrogels as reported by Vahdati et al. with similar grafted copolymers(Vahdati et al., 2020b). This phenomenon, that has been widely described in the literature for confined layers of various fluids(Ben Amar, Bonn, Amar, & Bonn, 2005; Biggins, Wei, Mahadevan, & Biggins, 2015; Nase, Derks, & Lindner, 2011), also holds for soft elastic solids where fingering instabilities maximize the compliance of the layer. As discussed by Shull and Creton(Shull et al., 2004), bulk fingering is expected in confined layers of soft elastic solids for high level of confinement $a_0/h_0 > 1$ and relatively large ratios of atmospheric pressure to Young's modulus ($P_0/E \gg 1$) which prevents

the formation of internal cavities. These finger-like instabilities can propagate along the interface, when adhesion is weak, or in the bulk when adhesion is strong.

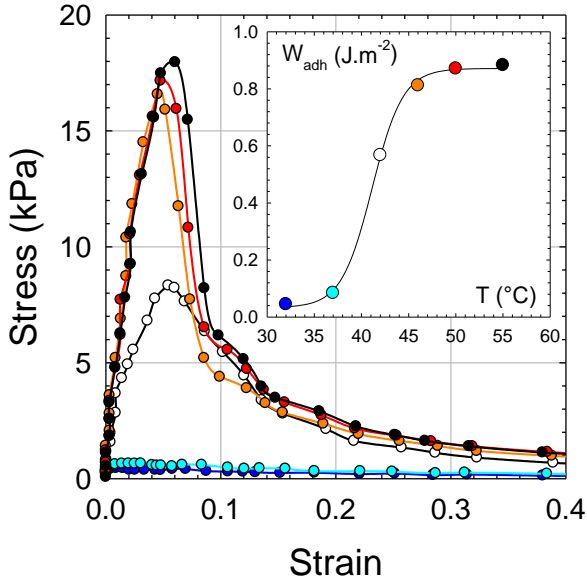


Figure 10

Temperature dependence of the adhesive behavior of HA-g-P100 prepared at 5 wt% in PBS:
 $T = 32\text{ }^{\circ}C$ (●), $37\text{ }^{\circ}C$ (●), $42\text{ }^{\circ}C$ (○), $46\text{ }^{\circ}C$ (●), $50\text{ }^{\circ}C$ (●) and $55\text{ }^{\circ}C$ (●).

The stress-strain curves are averages based on triplicates.
 The work of adhesion (W_{adh}) is proportional to the area under the stress strain curve.

At higher temperatures $T = 50$ and $55^{\circ}C$, the initial slope of the curve is well described by equation [3]. Nevertheless, there is an increasing deviation from the theoretical behavior with increasing strain that can be ascribed to a more progressive development of the fingering instabilities giving rise to a more rounded shape of the tack curve.

These instabilities, which appear around the peak in nominal stress at the adhesive-air interface for $\epsilon < 0.1$, grow into the bulk, moving from the edge of the confined layer toward the center as the probe is pulled up, and lead to a large drop in stress. Upon stretching, the confined hydrogel layer continually softens as shown by the regular decrease in the nominal stress which becomes negligible beyond $\epsilon = 1$. As described by Vahdati et al. with poly(N,N-dimethylacrylamide) (PDMA) grafted with PNIPAM side chains, the softening behavior can be attributed to the pull-out under strain of PNIPAM grafts from hydrophobic domains bridging hydrophilic backbones (Vahdati et al., 2020b). From these curves, the work of adhesion (W_{adh}) can be calculated by multiplying the area under the nominal stress-strain curve up to failure by the initial thickness:

$W_{adh} = h_0 \times \int_0^{\epsilon_{max}} \sigma(\epsilon) d\epsilon$. As shown in the inset of **Figure 10**, the work of adhesion

follows the general trend of the thermo-thickening behavior with a large increase of adhesive properties correlated to the sol/gel transition. The maximum values obtained for such formulations at 5 wt%, around 1 J/m^2 , are far below usual pressure sensitive adhesive (PSA) but we have to consider that here the formulation contains 95 wt% of water.

In the case of the HA-g-P50 formulation studied in the gel regime ($T = 25 \text{ }^\circ\text{C}$), the stress-strain curve given in **Figure 11** displays an initial slope at low strain ($\varepsilon < 0.1$) which is similar to that of HA-g-P100 studied at $55 \text{ }^\circ\text{C}$. This result is in agreement with their close elastic modulus which were determined under the same conditions: 1200 and 1140 Pa, respectively.

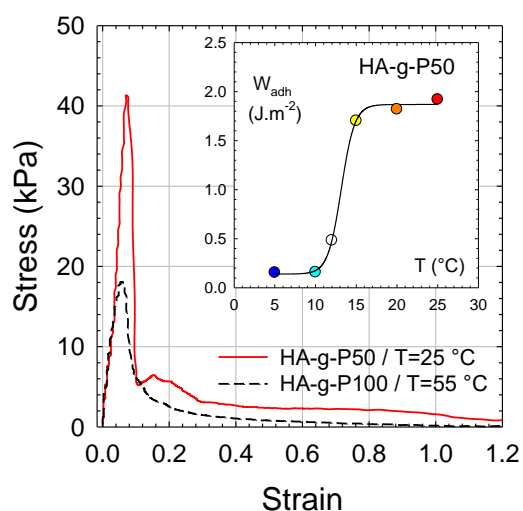


Figure 11

Adhesive properties in the gel regime of HA-g-P50 ($T = 25 \text{ }^\circ\text{C}$) and HA-g-P100 ($T = 55 \text{ }^\circ\text{C}$); $C = 5 \text{ wt\%}$ in PBS.

Inset: Temperature dependence of the adhesive behavior of HA-g-P50 ($C = 5 \text{ wt\%}$ in PBS) :

$T = 5 \text{ }^\circ\text{C}$ (●), $10 \text{ }^\circ\text{C}$ (●), $12 \text{ }^\circ\text{C}$ (○), $15 \text{ }^\circ\text{C}$ (●), $20 \text{ }^\circ\text{C}$ (●) and $25 \text{ }^\circ\text{C}$ (●).

The stress-strain curves are averages based on triplicates.

Nevertheless, one can observe clear differences between these two samples with: (i) a much higher resistance to deformation with a maximum stress at 40 kPa for HA-g-P50, compared to 18 kPa for HA-g-P100, (ii) an abrupt decrease of the stress for $\varepsilon > 0,07$ followed by a second peak stress of low amplitude and a pseudo plateau which extends up to $\varepsilon = 1.2-1.4$ giving rise to a higher work of adhesion ($W_{\text{adh}} \cong 2 \text{ J.m}^{-2}$) compared to HA-g-P100 ($W_{\text{adh}} \cong 0.9 \text{ J.m}^{-2}$).

These features, which highlight a greater elastic contribution of HA-g-P50 during deformation, can be attributed to a stronger cohesion of P50 domains, compared to P100 ones, thus offering a greater resistance to the pull out of LCST grafts under strain from hydrophobic domains bridging hydrophilic backbones. Moreover, it can be assumed that the higher level of entanglement of HA-

g-P50 chains also contributes to the reinforcement of viscoelastic properties at large deformations.

3.3.5. Injectability

For a proof of concept, injectability tests were performed by injecting HA-g-P100 and HA-g-P50 solutions (C=5 wt%), initially stored below their gelation temperatures, into a PBS bath thermostated either below or above the gel point. The tests were carried out with syringes of 1 mL ($R_s = 2.3$ mm) equipped with 35G needle ($R_n = 0.13$ mm ; $L_n = 12.7$ mm) commonly used in cases of self-injection.

In the case of HA-g-P100, which exhibits a sol/gel transition at 35 °C, the viscous solution at room temperature is rapidly dispersed when injected into the PBS bath at 20 °C and leads to a fast release of Rhodamine (see **Video 1** in supplementary information). Conversely, when the same solution is injected into the PBS bath at 37 °C, just above the gelation point, one can observe the instantaneous formation of an extruded gel filament which remains stable and greatly slows down the Rhodamine release.

In the case of HA-g-P100, the injection force was also measured as a function of injection rate using a specific setup mounted on an Instron machine (see **Figure S7** in supporting information). By increasing the injection rate between 10 and 200 mm/min, corresponding to flow rates between 0.18 and 3.7 mL/min, the force increases from 2.2 N to 5.7 N (see **Figure S8** in supporting information) but remains well below the limit of 12 N which is considered by patients as a boundary condition for an easy injection. (Robinson et al., 2020)

In the case of the solution of HA-g-P50 (C=5 wt%), which displays a gelation temperature at 10 °C, the tests were performed by hand at 5 and 20 °C (see **Video 2** in supporting information) and similar behaviors were observed with rapid dissolution at 5 °C and formation of a stable gel filament at 20 °C. Nevertheless, these tests remain qualitative because in the first case ($T < T_{gel}$) the syringe must be immersed in the PBS bath equilibrated with ice at 5° C to avoid gelation before the injection. This particular situation is observed during the test carried out in the PBS

bath at 20°C, when the syringe is not thermostated below 10°C ; this leading to very high injection forces.

This general comparison between the two copolymers, highlights the impact of the physico-chemical parameters playing a key role on gelation and injection properties. The size of the macromolecular backbone indeed directly impacts the viscosity and the injectability at low temperature but this can be controlled with the copolymer concentration. By decreasing the gelation temperature, it is possible to form gels that are more stable under physiological conditions, but in this case the injection must be carried out at low temperature. This can be considered for example in the case of tissue engineering by introducing stem cells into a liquid matrix at low temperature before letting them proliferate and differentiate under physiological conditions. In the case of direct introduction or injection into the human body, the gelation temperature must remain above room temperature to avoid gelation before introduction. In this case an important point to consider is the sharpness of the transition which is closely dependent on the thermodynamic properties of the reactive stickers.

4. Conclusions

The grafting of LCST side-chains onto water-soluble backbones is a versatile method for the preparation of responsive copolymers with orchestrable sol/gel transition properties. In this context, the use of poly(*N*-alkylacrylamide)s characterized by a phase transition close to body temperature are triggers of choice for the development of applications in bioengineering. Starting from PNIPAM responsive polymers, the incorporation of a hydrophobic comonomer, NtBAM, allows easy adjustment of the transition temperature below 35 °C. The introduction of increasing amounts of NtBAM decreases the transition temperature in aqueous medium but also the dynamics of the aggregates as revealed by the increase in hysteresis during the cooling step. Once grafted onto the hyaluronan backbone, LCST side-chains begin to self-associate into microdomains at temperatures similar to those of the ungrafted chains. The main difference comes from the lower transition enthalpy of the grafts which underlines a less effective

dehydration process (breaking of water/monomer hydrogen bonds in favor of monomer/monomer interactions). In the semi-dilute entangled regime, the formulations exhibit a clear sol/gel transition with a large increase of their viscoelastic properties. In the gel regime, the elastic properties are controlled by the responsive stickers which serve as physical crosslinks but also by the molar mass of the copolymer which impacts the level of entanglement of the network. The formation of elastic gels is also coupled with a strong increase in adhesion properties and a very good resistance to dissolution when immersed in an excess of solvent above T_{gel} .

If the structure/properties relationships are considered, it is interesting to discuss separately the role of responsive grafts on the one hand and of the water-soluble backbone on the other hand.

When choosing a LCST trigger, there are at least 3 main characteristics to consider:

1) The transition temperature. It can easily be adjusted by modifying the hydrophilic/hydrophobic balance of the LCST chain. Nevertheless, the dependence of the transition temperature on the concentration, which can vary greatly from one polymer to another, is also important to consider if precise control of the transition zone is sought.

2) The sharpness of the transition. It is essentially based on the phase diagram of the LCST polymer in the solvent considered, i.e. on the variation of the concentration of polymer-rich and solvent-rich phases with temperature.

3) The dynamics of LCST microdomains forming crosslinks. It depends on polymer hydrophobicity but also on how far is the polymer-rich phase from its glass transition. This will strongly influence the lifetime of the association and of the entire polymer network.

Regarding the water-soluble backbone, the two main characteristics are its hydrophilicity and its molar mass. In the case of copolymers characterized by a high level of modification, as is the case in the present study, the backbone must be very soluble in water in order to avoid macro-phase separation above the transition temperature. The molar mass, and therefore the level of chain entanglement, is also important as it improves the elastic properties in the linear regime. At large deformations, which have been little studied so far, we believe this may be a critical parameter because the deformation and flow of the main chain by reptation requires the

dissociation of LCST stickers and the longer the chain, the greater the number of grafted stickers will slow down its reptation.

If we look at the literature dealing with thermoassociative copolymers it appears that the nature of responsive grafts critically influences the association temperature as well as the dynamics of the physical network. This has been shown for example with various polymeric backbones, such as poly(sodium acrylate){Durand, 2000 #408}{Podhajecka, 2007 #391} or alginates{Safakas, 2021 #484}, by modifying the hydrophilic/hydrophobic balance of the side-chains. From our expertise on thermoassociating polymers, it appears that for a given LCST side-chain, the main parameters controlling the viscoelastic properties in the semi-dilute entangled regime are the level of entanglement of the copolymer chain (C/C_e) and the weight fraction of LCST grafts. All these points are important and deserve to be studied in more details in future investigations in order to properly control all of the properties sought in applications relating to injectable hydrogels.

Acknowledgements

Lucile Barbier and Marine Protat contributed equally to this work. The authors gratefully acknowledge the financial support from CNRS, ESPCI Paris and Sorbonne University for the PhD funding of Lucile Barbier (Doctoral School on Materials Science ED397) and the Master funding of Marine Protat (Appel à Projets Convergence Sorbonne University). The authors also thank Dr. G. Ducouret from the SIMM lab. for technical advice on performing rheological measurements and Dr. P. R. Rajamohanam from NCL Pune (India) for carrying out temperature NMR experiments.

References

- Alhadithi, T. S. R., Barnes, H. A., Walters, K., Al-Hadithi, T. S. R., Barnes, H. A., & Walters, K. (1992). The relationship between the linear (oscillatory) and nonlinear (steady-state) flow properties of a series of polymer and colloidal systems. *Colloid & polymer science*, 270(1), 40-46.
- Arvidson, S. A., Lott, J. R., Brackhagen, M., Arvidson, S. A., Lott, J. R., McAllister, J. W., . . . Brackhagen, M. (2013). Interplay of Phase Separation and Thermoreversible Gelation in Aqueous Methylcellulose Solutions. *Macromolecules*, 46(1), 300-309.
- Aseyev, V., Tenhu, H., & Winnik, F. M. (2011). Non-ionic Thermoresponsive Polymers in Water. *Self Organized Nanostructures of Amphiphilic Block Copolymers II*, 242, 29-89.
- Bellotti, E., Schilling, A. L., Little, S. R., & Decuzzi, P. (2021). Injectable thermoresponsive hydrogels as drug delivery system for the treatment of central nervous system disorders: A review. *Journal of Controlled Release*, 329, 16-35.
- Ben Amar, M., Bonn, D., Amar, M. B., & Bonn, D. (2005). Fingering instabilities in adhesive failure. *Physica . D . Nonlinear phenomena*, 209(1-4), 1-16.
- Biggins, J. S., Wei, Z., Mahadevan, L., & Biggins, J. S. (2015). Fluid-driven fingering instability of a confined elastic meniscus. *Europhysics letters : EPL (EDP Sciences)*, 110(3), 34001.
- Boateng, J. S., Matthews, K. H., Stevens, H. N. E., & Eccleston, G. M. (2008). Wound Healing Dressings and Drug Delivery Systems: A Review. *Journal of Pharmaceutical Sciences*, 97(8), 2892-2923.
- Bouttier, S., Yeo, A., Any-Grah, A., Geiger, S., Huang, N., Nicolas, V., . . . Gnanan, K. C. N. (2020). Characterization and in vitro evaluation of a vaginal gel containing *Lactobacillus crispatus* for the prevention of gonorrhoea. *International Journal of Pharmaceutics*, 588.
- Bromberg, L. (1998). Scaling of rheological properties of hydrogels from associating polymers. *Macromolecules*, 31(18), 6148-6156.
- Brown, W., Schillen, K., & Hvidt, S. (1992). Triblock copolymers in aqueous-solution studied by static and dynamic light-scattering and oscillatory shear measurements - influence of relative block sizes. *Journal of Physical Chemistry*, 96(14), 6038-6044.
- Cao, C., Yan, C. H., Hu, Z. Q., & Zhou, S. (2015). Potential application of injectable chitosan hydrogel treated with siRNA in chronic rhinosinusitis therapy. *Molecular Medicine Reports*, 12(5), 6688-6694.
- Clark, A. H., & Farrer, D. B. (1995). Kinetics of biopolymer gelation—Implications of a cascade theory description for the concentration, molecular weight, and temperature dependences of the shear modulus and gel time. *Journal of Rheology*, 39(6), 1429-1444.
- Clark, A. H., & Ross-Murphy, S. B. (1985). The concentration dependence of biopolymer gel modulus. *British Polymer Journal*, 17(2), 164-168.
- Colby, R. H. (2010). Structure and linear viscoelasticity of flexible polymer solutions: comparison of polyelectrolyte and neutral polymer solutions. *Rheologica Acta*, 49(5), 425-442.
- D'Este, M., Alini, M., & Eglin, D. (2012). Single step synthesis and characterization of thermoresponsive hyaluronan hydrogels. *Carbohydrate Polymers*, 90(3), 1378-1385.
- D'Este, M., Sprecher, C. M., Milz, S., Nehrbass, D., Dresing, I., Zeiter, S., . . . Eglin, D. (2016). Evaluation of an injectable thermoresponsive hyaluronan hydrogel in a rabbit osteochondral defect model. *Journal of Biomedical Materials Research Part A*, 104(6), 1469-1478.
- Desbrieres, J., Hirrien, M., & Ross-Murphy, S. B. (2000). Thermogelation of methylcellulose: rheological considerations. *Polymer*, 41(7), 2451-2461.
- Destruel, P. L., Zeng, N., Maury, M., Mignet, N., & Boudy, V. (2017). In vitro and in vivo evaluation of in situ gelling systems for sustained topical ophthalmic delivery: state of the art and beyond. *Drug Discovery Today*, 22(4), 638-651.

- Durand, A., & Hourdet, D. (1999). Synthesis and thermoassociative properties in aqueous solution of graft copolymers containing poly(N-isopropylacrylamide) side chains. *Polymer*, 40(17), 4941-4951.
- Durand, A., & Hourdet, D. (2000). Thermoassociative graft copolymers based on poly(N-isopropylacrylamide): Relation between the chemical structure and the rheological properties. *Macromolecular Chemistry and Physics*, 201(8), 858-868.
- Ekerdt, B. L., Fuentes, C. M., Lei, Y. G., Adil, M. M., Ramasubramanian, A., Segalman, R. A., & Schaffer, D. V. (2018). Thermoreversible Hyaluronic Acid-PNIPAAm Hydrogel Systems for 3D Stem Cell Culture. *Advanced Healthcare Materials*, 7(12).
- Flory, P. J. (1941). Molecular Size Distribution in Three Dimensional Polymers. I. Gelation 1. *Journal of the American Chemical Society*, 63(11), 3083-3090.
- Gibbons, O., Carroll, W. M., Aldabbagh, F., & Yamada, B. (2006). Nitroxide-mediated controlled statistical copolymerizations of N-isopropylacrylamide with N-tert-butylacrylamide. *Journal of Polymer Science Part a-Polymer Chemistry*, 44(21), 6410-6418.
- Guo, H., Brulet, A., Rajamohanam, P. R., Marcellan, A., Sanson, N., & Hourdet, D. (2015). Influence of topology of LCST-based graft copolymers on responsive assembling in aqueous media. *Polymer*, 60, 164-175.
- Guo, H., Goncalves, M. D., Ducouret, G., & Hourdet, D. (2018). Cold and Hot Gelling of Alginate-graft-PNIPAM: a Schizophrenic Behavior Induced by Potassium Salts. *Biomacromolecules*, 19(2), 576-587.
- Ha, D. I., Lee, S. B., Chong, M. S., Lee, Y. M., Kim, S. Y., & Park, Y. H. (2006). Preparation of thermo-responsive and injectable hydrogels based on hyaluronic acid and poly(N-isopropylacrylamide) and their drug release behaviors. *Macromolecular Research*, 14(1), 87-93.
- Hermans Jr, J. (1965). Investigation of the elastic properties of the particle network in gelled solutions of hydrocolloids. I. Carboxymethyl cellulose. *Journal of Polymer Science Part A: General Papers*, 3(5), 1859-1868.
- Hermanson, G. T. (1996). Modification with synthetic polymers. *Bioconjugate techniques*, 605-629.
- Heymann, E. (1935). Studies on sol-gel transformations. I. The inverse sol-gel transformation of methylcellulose in water. *Transactions of the Faraday Society*, 31(1), 0846-0863.
- Hoffman, A. S., Stayton, P. S., Bulmus, V., Chen, G. H., Chen, J. P., Cheung, C., . . . Miyata, T. (2000). Really smart bioconjugates of smart polymers and receptor proteins. *Journal of Biomedical Materials Research*, 52(4), 577-586.
- Hourdet, D., Durand, A., & Herve, M. (1999). Reversible gelation of aqueous polymer solutions induced by responsive stickers. *Abstracts of Papers of the American Chemical Society*, 218, U404-U405.
- Hourdet, D., L'Alloret, F., Durand, A., Lafuma, F., Audebert, R., & Cotton, J. P. (1998). Small-angle neutron scattering study of microphase separation in thermoassociative copolymers. *Macromolecules*, 31(16), 5323-5335.
- Hourdet, D., Lalloret, F., & Audebert, R. (1994). Reversible thermothickening of aqueous polymer-solutions. *Polymer*, 35(12), 2624-2630.
- Iatridi, Z., Saravanou, S.-F., & Tsitsilianis, C. (2019). Injectable self-assembling hydrogel from alginate grafted by P(N-isopropylacrylamide-co-N-tert-butylacrylamide) random copolymers. *Carbohydrate Polymers*, 219, 344-352.
- Irie, M. (1993). Stimuli-Responsive Poly(N-Isopropylacrylamide) - Photoinduced and Chemical-Induced Phase-Transitions. *Advances in Polymer Science*, 110, 49-65.
- Karakasyan, C., Lack, S., Brunel, F., Maingault, P., & Hourdet, D. (2008). Synthesis and rheological properties of responsive thickeners based on polysaccharide architectures. *Biomacromolecules*, 9(9), 2419-2429.
- Koffi, A. A., Agnely, F., Ponchel, G., & Grossiord, J. L. (2006). Modulation of the rheological and mucoadhesive properties of thermosensitive poloxamer-based hydrogels intended for

- the rectal administration of quinine. *European Journal of Pharmaceutical Sciences*, 27(4), 328-335.
- Kokufuta, E., Zhang, Y. Q., Tanaka, T., & Mamada, A. (1993). Effects of Surfactants on the Phase-Transition of Poly(N-Isopropylacrylamide) Gel. *Macromolecules*, 26(5), 1053-1059.
- Krause, W. E., Bellomo, E. G., & Colby, R. H. (2001). Rheology of sodium hyaluronate under physiological conditions. *Biomacromolecules*, 2(1), 65-69.
- L'Alloret, F. (2006). Polymer comprising water-soluble units and LCST units, and aqueous composition comprising same. In S. United (Ed.): LOreal SA.
- Leibler, L., Rubinstein, M., Colby, R. H., Leibler, L., Rubinstein, M., & Colby, R. H. (1991). Dynamics of reversible networks. *Macromolecules*, 24(16), 4701-4707.
- Liu, H. Y., & Zhu, X. X. (1999). Lower critical solution temperatures of N-substituted acrylamide copolymers in aqueous solutions. *Polymer*, 40(25), 6985-6990.
- Malafaya, P. B., Silva, G. A., & Reis, R. L. (2007). Natural-origin polymers as carriers and scaffolds for biomolecules and cell delivery in tissue engineering applications. *Advanced Drug Delivery Reviews*, 59(4-5), 207-233.
- Maroy, P., Hourdet, D., L'Alloret, F., & Audebert, R. (1998). Thermoviscosifying polymers, their synthesis and their uses in particular in the oil industry. In U. European (Ed.): Sofitech NV.
- Milas, M., Rinaudo, M., Roure, I., Al-Assaf, S., Phillips, G. O., & Williams, P. A. (2001). Comparative rheological behavior of hyaluronan from bacterial and animal sources with cross-linked hyaluronan (hylan) in aqueous solution. *Biopolymers*, 59(4), 191-204.
- Miura, Y., Tsuji, Y., Cho, R., Fujisawa, A., Fujisawa, M., Kamata, H., . . . Koike, K. (2021). The feasibility of a novel injectable hydrogel for protecting artificial gastrointestinal ulcers after endoscopic resection: an animal pilot study. *Scientific Reports*, 11(1).
- Mortensen, K., Brown, W., & Jorgensen, E. (1994). Phase-behavior of poly(propylene oxide) poly(ethylene oxide) poly(propylene oxide) triblock copolymer melt and aqueous-solutions. *Macromolecules*, 27(20), 5654-5666.
- Mortisen, D., Peroglio, M., Alini, M., & Eglin, D. (2010). Tailoring Thermoreversible Hyaluronan Hydrogels by "Click" Chemistry and RAFT Polymerization for Cell and Drug Therapy. *Biomacromolecules*, 11(5), 1261-1272.
- Muramatsu, K., Saito, Y., Wada, T., Hirai, H., & Miyawaki, F. (2012). Poly(N-isopropylacrylamide-co-N-tert-butylacrylamide)- grafted hyaluronan as an injectable and self-assembling scaffold for cartilage tissue engineering. *Journal of Biomedical Science and Engineering*, 05(11), 639-646.
- Nakajima, N., & Ikada, Y. (1995). Mechanism of amide formation by carbodiimide for bioconjugation in aqueous-media. *Bioconjugate Chemistry*, 6(1), 123-130.
- Nase, J., Derks, D., & Lindner, A. (2011). Dynamic evolution of fingering patterns in a lifted Hele-Shaw cell. *Physics of Fluids*, 23(12), 123101.
- Neises, B., & Steglich, W. (1978). 4-Dialkylaminopyridines as Acylation Catalysts .5. Simple Method for Esterification of Carboxylic-Acids. *Angewandte Chemie-International Edition in English*, 17(7), 522-524.
- Obukhov, S. P., Rubinstein, M., Colby, R. H., Obukhov, S. P., Rubinstein, M., & Colby, R. H. (1994). Network Modulus and Superelasticity. *Macromolecules*, 27(12), 3191-3198.
- Ohya, S., Nakayama, Y., & Matsuda, T. (2001). Thermoresponsive artificial extracellular matrix for tissue engineering: Hyaluronic acid bioconjugated with poly(N-isopropylacrylamide) grafts. *Biomacromolecules*, 2(3), 856-863.
- Peroglio, M., Eglin, D., Benneker, L. M., Alini, M., & Grad, S. (2013). Thermoreversible hyaluronan-based hydrogel supports in vitro and ex vivo disc-like differentiation of human mesenchymal stem cells. *Spine Journal*, 13(11), 1627-1639.
- Peroglio, M., Grad, S., Mortisen, D., Sprecher, C. M., Illien-Jünger, S., Alini, M., & Eglin, D. (2012). Injectable thermoreversible hyaluronan-based hydrogels for nucleus pulposus cell encapsulation. *European spine journal : official publication of the European Spine*

- Society, the European Spinal Deformity Society, and the European Section of the Cervical Spine Research Society*, 21 Suppl 6(Suppl 6), S839-S849.
- Pitarresi, G., Fiorica, C., Licciardi, M., Palumbo, F. S., & Giammona, G. (2013). New hyaluronic acid based brush copolymers synthesized by atom transfer radical polymerization. *Carbohydrate Polymers*, 92(2), 1054-1063.
- Ramya, K. A., Kodavaty, J., Dorishetty, P., Setti, M., & Deshpande, A. P. (2019). Characterizing the yielding processes in pluronic-hyaluronic acid thermoreversible gelling systems using oscillatory rheology. *Journal of Rheology*, 63(2), 215-228.
- Robinson, T. E., Hughes, E. A. B., Bose, A., Cornish, E. A., Teo, J. Y., Eisenstein, N. M., . . . Cox, S. C. (2020). Filling the Gap: A Correlation between Objective and Subjective Measures of Injectability. *Advanced Healthcare Materials*, 9(5).
- Rochas, C., Rinaudo, M., Landry, S., Rochas, C., Rinaudo, M., & Landry, S. (1989). Relation between the molecular structure and mechanical properties of carrageenan gels. *Carbohydrate Polymers*, 10(2), 115-127.
- Rosenzweig, D. H., Fairag, R., Mathieu, A. P., Li, L., Eglin, D., D'Este, M., . . . Haglund, L. (2018). Thermoreversible hyaluronan-hydrogel and autologous nucleus pulposus cell delivery regenerates human intervertebral discs in an ex vivo, physiological organ culture model. *European Cells & Materials*, 36, 200-217.
- Rubinstein, M., & Colby, R. H. (2007). *Polymer physics / Michael Rubinstein and Ralph H. Colby*. Oxford :: Oxford University Press.
- Rubinstein, M., & Semenov, A. N. (2001). Dynamics of entangled solutions of associating polymers. *Macromolecules*, 34(4), 1058-1068.
- Safakas, K., Saravanou, S.-F., Iatridi, Z., & Tsitsilianis, C. (2021). Alginate-g-PNIPAM-Based Thermo/Shear-Responsive Injectable Hydrogels: Tailoring the Rheological Properties by Adjusting the LCST of the Grafting Chains. *International Journal of Molecular Sciences* (Vol. 22).
- Shibayama, M., Ikkai, F., Inamoto, S., Nomura, S., & Han, C. C. (1996). pH and salt concentration dependence of the microstructure of poly(N-isopropylacrylamide-co-acrylic acid) gels. *Journal of Chemical Physics*, 105(10), 4358-4366.
- Shibayama, M., Morimoto, M., & Nomura, S. (1994). Phase-Separation Induced Mechanical Transition of Poly(N-Isopropylacrylamide) Water Isochore Gels. *Macromolecules*, 27(18), 5060-5066.
- Shull, K. R., Creton, C., Shull, K. R., & Creton, C. (2004). Deformation behavior of thin, compliant layers under tensile loading conditions. *Journal of polymer science.*, 42(22), 4023-4043.
- Smart, J. D. (2005). The basics and underlying mechanisms of mucoadhesion. *Advanced Drug Delivery Reviews*, 57(11), 1556-1568.
- Soyarslan, C., Pradas, M., & Bargmann, S. (2019). Effective elastic properties of 3D stochastic bicontinuous composites. *Mechanics of Materials*, 137, 103098.
- Staros, J. V., Wright, R. W., & Swingle, D. M. (1986). Enhancement by N-hydroxysulfosuccinimide of water-soluble carbodiimide-mediated coupling reactions. *Analytical Biochemistry*, 156(1), 220-222.
- Stockmayer, W. H. (1943). Theory of Molecular Size Distribution and Gel Formation in Branched-Chain Polymers. *The Journal of Chemical Physics*, 11(2), 45-55.
- Sun, P., Li, B., Wang, Y., Ma, J., Ding, D., & He, B. (2003). ¹H NMR studies of poly(N-isopropylacrylamide) gels near the phase transition. *European Polymer Journal*, 39(5), 1045-1050.
- Suto, S., Nishibori, W., Kudo, K., & Karasawa, M. (1989). Lyotropic liquid-crystalline solutions of hydroxypropyl cellulose in water - effect of salts on the turbidity and viscometric behavior. *Journal of Applied Polymer Science*, 37(3), 737-749.
- Suzuki, A. (1993). Phase-Transition in Gels of Submillimeter Size Induced by Interaction with Stimuli. *Advances in Polymer Science*, 110, 199-240.

- Thambi, T., Phan, V. H. G., & Lee, D. S. (2016). Stimuli-Sensitive Injectable Hydrogels Based on Polysaccharides and Their Biomedical Applications. *Macromolecular Rapid Communications*, 37(23), 1881-1896.
- Vahdati, M., Ducouret, G., Creton, C., & Hourdet, D. (2020a). Thermally Triggered Injectable Underwater Adhesives. *Macromolecular Rapid Communications*, 41(7).
- Vahdati, M., Ducouret, G., Creton, C., & Hourdet, D. (2020b). Topology-Specific Injectable Sticky Hydrogels. *Macromolecules*, 53(22), 9779-9792.
- Yeung, D. W. K., Liu, L. Z., Langlois, B. R. C., Charmot, D., & Corpart, P. (2001). Polymers which exhibit thermo-thickening properties and process making same. In U. European (Ed.): Rhodia Inc.
- Zeng, N., Seguin, J., Destruel, P. L., Dumortier, G., Maury, M., Dhotel, H., . . . Boudy, V. (2017). Cyanine derivative as a suitable marker for thermosensitive in situ gelling delivery systems: In vitro and in vivo validation of a sustained buccal drug delivery. *International Journal of Pharmaceutics*, 534(1-2), 128-135.
- Zhang, Y. Q., Tanaka, T., & Shibayama, M. (1992). Super-Absorbency and Phase-Transition of Gels in Physiological Salt-Solutions. *Nature*, 360(6400), 142-144.